PHYSICAL REVIEW E **94**, 022130 (2016)

Explicit densities of multidimensional ballistic Lévy walks

Marcin Magdziarz* and Tomasz Zorawik
Faculty of Pure and Applied Mathematics, Hugo Steinhaus Center, Wroclaw University of Science and Technology, Wyspianskiego 27, 50-370 Wroclaw, Poland

(Received 5 March 2016; revised manuscript received 14 June 2016; published 22 August 2016)

Lévy walks have proved to be useful models of stochastic dynamics with a number of applications in the modeling of real-life phenomena. In this paper we derive explicit formulas for densities of the two- (2D) and three-dimensional (3D) ballistic Lévy walks, which are most important in applications. It turns out that in the 3D case the densities are given by elementary functions. The densities of the 2D Lévy walks are expressed in terms of hypergeometric functions and the right-side Riemann-Liouville fractional derivative, which allows us to efficiently evaluate them numerically. The theoretical results agree perfectly with Monte Carlo simulations.

DOI: 10.1103/PhysRevE.94.022130

I. INTRODUCTION

Starting with pioneering papers [1,2] Lévy walks have become useful models of anomalous stochastic dynamics. They have found interesting applications in various real-life phenomena and complex systems. The commonly quoted examples are blinking nanocrystals [3], light transport in optical materials [4], foraging patterns of animals [5–7], epidemic spreading [8,9], fluid flow in a rotating annulus [10], and human travel [11,12]. Recently Lévy walks have been used to describe migration of swarming bacteria [13]. For more examples we refer to the recent review [14], which is also a good introduction to the topic.

In the standard formulation of the Lévy walk there is a strong coupling between the traveled distance and the duration of the flight [15,16]. In the simplest setting the Lévy walker performs a motion with constant speed v, and its trajectories are continuous and piecewise linear. As a result of the above mentioned coupling we get that the mean square displacement of the Lévy walk is finite [2], even in the case of power-law jump distribution (intuitively, long jumps are penalized by requiring more time to be performed). This is very different from Lévy flight, which is another popular model of superdiffusion and has infinite mean square displacement [15–17].

In this paper we derive explicit probability density functions (PDFs) of the two- (2D) and three-dimensional (3D) ballistic Lévy walk limits. In the 3D case the PDF is given by elementary functions. For the 2D Lévy walk its PDF is expressed using hypergeometric functions and the Riemann-Liouville derivative, which can be efficiently evaluated numerically. Moreover these PDFs solve certain differential equations [18] with the fractional material derivative [19,20]. The main idea of this paper is to relate the multidimensional PDF to a proper one-dimensional (1D) distribution using methods from Ref. [21] and then apply the formula of Godrèche and Luck [22] to invert the Fourier-Laplace transform. It should be underlined that the densities of 1D ballistic Lévy walks have been recently found by Froemberg *et al.* [23].

*marcin.magdziarz@pwr.edu.pl

II. EXPLICIT DENSITIES

Let us recall the formal definition of a d-dimensional Lévy walk. Consider a sequence of independent, identically distributed (IID) positive random variables $T_1,T_2,\dots$, representing the consecutive waiting times of the walker. We assume that the distribution of waiting times is power-law, $\psi(t)\propto t^{-1-\alpha},\alpha\in(0,1)$. Denote by $N(t)=\max\{k\geqslant 0:\sum_{i=1}^k T_i\leqslant t\}$ the corresponding process counting the number of jumps up to time t. Next, let us define the jumps of the walker

$$\mathbf{X}_i = vT_i\mathbf{V}_i,\quad i=1,2,\dots .$$

Here $\mathbf{V}_1,\mathbf{V}_2,\dots$ is a sequence of IID random unit vectors distributed uniformly on the d-dimensional sphere $\mathbb{S}^d$. Each vector $\mathbf{V}_i$ governs the direction of ith jump. The constant v is the speed; for simplicity we assume that $v=1$. It is clear from the definition that the length of each jump $\|\mathbf{X}_i\|$ is equal to the length of the corresponding waiting time T_i. Such spatiotemporal coupling is typical for Lévy walks. Now, the so-called undershooting Lévy walk is defined as $\mathbf{L}_{ULW}(t)=\sum_{i=1}^{N_t}\mathbf{X}_i$. The trajectories of this process are piecewise constant and have jumps, thus they are not continuous. However, applying simple linear interpolation on the trajectories of $\mathbf{L}_{ULW}(t)$, we arrive at the final definition of the standard Lévy walk $\mathbf{L}(t)$:

$$\mathbf{L}(t)=\sum_{i=1}^{N(t)}T_i\mathbf{V}_i+\left(t-\sum_{i=1}^{N(t)}T_i\right)\mathbf{V}_{N(t)+1}. \tag{1}$$

The trajectories of the Lévy walk $\mathbf{L}(t)$ are continuous and piecewise linear (motion with constant speed). Moreover, due to the spatiotemporal coupling its mean square displacement is finite. $\mathbf{L}(t)$ is a d-dimensional process, so we can write it as a vector $\mathbf{L}(t)=(L_1(t),\dots,L_d(t))$. Moreover, the distribution of $\mathbf{L}(t)$ is rotationally invariant; each direction of the motion is equally possible. It is the consequence of the fact that the jump directions $\mathbf{V}_i$ are uniformly distributed on the d-dimensional sphere $\mathbb{S}^d$. Therefore to determine the PDF of $\mathbf{L}(t)$ it is enough to determine the PDF of the radius $\|\mathbf{L}(t)\|=\sqrt{L_1^2(t)+\dots+L_d^2(t)}$. In what follows we will use two main ideas. The first one concerns determining the asymptotic PDF of $L_1(t)$, the projection of $\mathbf{L}(t)$ on the first axis. The second one is finding the relation between the asymptotic distributions of $\|\mathbf{L}(t)\|$ and $L_1(t)$.

The diffusion limit of $\mathbf{L}(t)$ has been recently established in Ref. [18]. Let us denote this limit process by $\mathbf{X}(t)$, which takes the form

$$\mathbf{X}(t) = \begin{cases} L_\alpha^-\big[S_\alpha^{-1}(t)\big] & \text{if } t \in \mathcal{R} \\ L_\alpha^-\big[S_\alpha^{-1}(t)\big] + \dfrac{t-G(t)}{H(t)-G(t)}\big\{L_\alpha\big[S_\alpha^{-1}(t)\big] - L_\alpha^-\big[S_\alpha^{-1}(t)\big]\big\} & \text{if } t \notin \mathcal{R}, \end{cases}$$

where $L_\alpha^-(t)$ is the left-continuous version of the d-dimensional α-stable Lévy motion L_α(t) with Fourier transform [17],

$$\begin{aligned}&\mathbf{E}\{\exp[i\langle k, L_\alpha(t)\rangle]\}\\ &= \exp\left\{t\int_{\mathbb{S}^d}|\langle k,s\rangle|^\alpha[i\,\mathrm{sgn}(\langle k,s\rangle)\tan(\pi\alpha/2)-1]K(ds)\right\},\end{aligned}$$

where $K(ds)$ is the uniform distribution on $\mathbb{S}^d$ and $\langle\ ,\ \rangle$ denotes the standard inner product in $\mathbb{R}^d$. Next, S_α(t) is the α-stable subordinator with Laplace transform [17]

$$\mathbf{E}\{\exp[-sS_\alpha(t)]\} = \exp\{-ts^\alpha\},$$

and $S_\alpha^{-1}(t) = \inf\{\tau \geqslant 0 : S_\alpha(\tau) > t\}$. Moreover

$$\mathcal{R} = \{S_\alpha(t) : t \geqslant 0\}, \quad G(t) = S_\alpha^-[S_\alpha^{-1}(t)],$$
$$H(t) = S_\alpha[S_\alpha^{-1}(t)].$$

Since $\mathbf{L}(t)$ is rotationally invariant, so is the limit $\mathbf{X}(t)$. In the following we will derive the explicit PDFs of $\mathbf{X}(t)$ in the 2D and 3D case.

A. 2D case

Denote the PDF of $\mathbf{X}(t) = (X_1(t), X_2(t))$ by $H(\mathbf{x},t), \mathbf{x} = (x_1,x_2) \in \mathbb{R}^2$. It follows from [18] that the Fourier-Laplace transform of $H(\mathbf{x},t)$ is given by

$$H(\mathbf{k},s) = \frac{1}{s}g\left(\frac{i\mathbf{k}}{s}\right) = \frac{1}{s}\frac{\int_{\mathbf{S}^2}\left(1-\langle\frac{i\mathbf{k}}{s},\mathbf{u}\rangle\right)^{\alpha-1}K(d\mathbf{u})}{\int_{\mathbf{S}^2}\left(1-\langle\frac{i\mathbf{k}}{s},\mathbf{u}\rangle\right)^{\alpha}K(d\mathbf{u})},$$

where $\mathbf{k} = (k_1,k_2) \in \mathbb{R}^2$ is the Fourier space variable, s is the Laplace space variable, and $K(d\mathbf{u})$ is the uniform distribution on the circle $\mathbf{S}^2$. Now we can notice that the Fourier-Laplace transform of the PDF of $X_1(t)$ is equal to $H_1(k_1,s) = H((k_1,0),s)$. The marginal distribution of the uniform distribution on a circle $K_1(d\mathbf{u})$ has the density [24]

$$K(du_1) = \frac{1}{\pi}\frac{1}{\left(1-u_1^2\right)^{1/2}}du_1; \tag{2}$$

thus $H_1(k_1,s) = \frac{1}{s}g_1(\frac{ik_1}{s})$, where

$$g_1(\xi) = \frac{\int_{-1}^1(1-\xi u)^{\alpha-1}\frac{1}{\pi(1-u^2)^{1/2}}du}{\int_{-1}^1(1-\xi u)^{\alpha}\frac{1}{\pi(1-u^2)^{1/2}}du}. \tag{3}$$

This corresponds to the scaling

$$H_1(x,t) = \frac{1}{t}\Phi_1\left(\frac{x}{t}\right), \tag{4}$$

where $x \in \mathbb{R}$. Now we are in position to apply the method of inverting a joined Fourier-Laplace transform from Refs. [22,23], which will allow us to get an explicit formula for Φ_1. This technique is based on a special representation of the function $g_1(\xi)$ and the Sokhotsky-Weierstrass theorem. We can write (see Appendix A)

$$g_1(\xi) = \mathbf{E}\frac{1}{1+\xi X_1(1)}, \tag{5}$$

and from the Sokhotsky-Weierstrass theorem we get (see Appendix B)

$$\Phi_1(x) = -\frac{1}{\pi}\lim_{\varepsilon\to 0}\mathrm{Im}\left[\frac{1}{x+i\varepsilon}\mathbf{E}\frac{1}{1-\frac{X_1(1)}{x+i\varepsilon}}\right]. \tag{6}$$

Now we combine Eqs. (5) and (6) and get the formula for Φ_1:

$$\Phi_1(x) = -\frac{1}{\pi}\lim_{\varepsilon\to 0}\mathrm{Im}\left[\frac{1}{x+i\varepsilon}g_1\left(-\frac{1}{x+i\varepsilon}\right)\right]. \tag{7}$$

This technique can be only applied for a 1D process operating in a ballistic regime whose Fourier-Laplace transform of PDF $p(t,x)$ has the scaling

$$p(k,s) = \frac{1}{s}r\left(\frac{ik}{s}\right). \tag{8}$$

It was originally developed by Godrèche and Luck [22] for inverting a double Laplace transform and then generalized by Froemberg *et al.* [23] for the Fourier-Laplace transform and use with ballistic Lévy walks. In our case g is given by Eq. (3). After some standard transformations we obtain

$$\Phi_1(x) = -\frac{1}{\pi|x|}\mathrm{Im}\frac{{}_2F_1\left([1-\alpha]/2, 1-\alpha/2; 1; \frac{1}{x^2}\right)}{{}_2F_1\left(-\alpha/2, [1-\alpha]/2; 1; \frac{1}{x^2}\right)} \tag{9}$$

for $x \in (-1,1)$ and $\Phi_1(x) = 0$ otherwise. Here ${}_2F_1(a,b;c;x)$ is the hypergeometric function [25] defined as

$${}_2F_1(a,b;c;x) = \sum_{k=0}^{\infty}\frac{(a)_k(b)_k}{(c)_k}\frac{x^k}{k!} \tag{10}$$

for $|x| < 1$ and analytically continued for $x > 1$. In this series $(a)_k = \frac{\Gamma[a+k]}{\Gamma[a]}$ is the Pochhammer symbol. The hypergeometric functions can be evaluated numerically and are implemented in most of the mathematical packages including Matlab and Mathematica. Their use ensures high-precision calculations.

We now relate the PDF $H_R(r,t)$ of the radius $\|\mathbf{X}(t)\|$ to the already calculated PDF of $X_1(t)$ using the method from Ref. [21]. The rotational invariance of Lévy walk $\mathbf{L}(t)$ implies the rotational invariance of the diffusion limit process $\mathbf{X}(t)$. Therefore to find $H(\mathbf{x},t)$ it suffices to determine $H_R(r,t)$. From the property $H(\mathbf{k},s) = \frac{1}{s}g(\frac{i\mathbf{k}}{s})$ we deduce the scaling $H_R(r,t) = \frac{1}{t}\Phi_R(\frac{r}{t})$. The factorization of $\mathbf{X}(1)$ into radial and directional parts gives us

$$\mathbf{X}(1) \overset{d}{=} \|\mathbf{X}(\mathbf{1})\|\mathbf{V}, \tag{11}$$

where $\mathbf{V}$ is a random vector uniformly distributed on a circle, independent of $\|\mathbf{X}(1)\|$, and "$\overset{d}{=}$" denotes the equality in

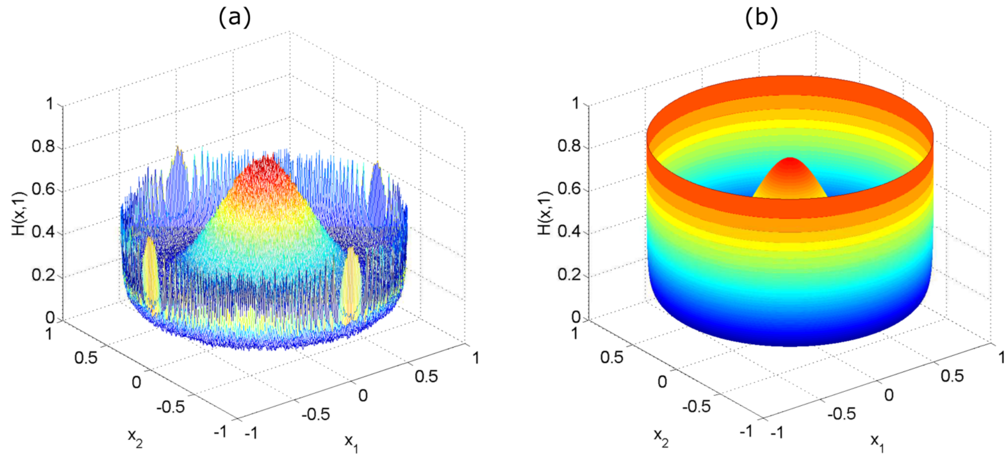

FIG. 1. Density $H(\mathbf{x},1)$ of 2D Lévy walk with $\alpha = 0.6$ estimated using Monte Carlo methods from 4×10^7 trajectories (a) and obtained from Eq. (17) (b).

distribution. This implies

$$\mathbf{P}(|X_1(1)| \leqslant x) = \frac{2}{\pi}\int_0^1 \frac{1}{(1-u^2)^{1/2}}\mathbf{P}\Big(\|\mathbf{X}(1)\| \leqslant \frac{x}{u}\Big)du \tag{12}$$

for $x \geqslant 0$. The differentiation of the above equation yields

$$\Phi_1(x) = \frac{1}{\pi}\int_0^1 \frac{1}{(1-u^2)^{1/2}}\frac{1}{u}\Phi_R\Big(\frac{x}{u}\Big)du, \tag{13}$$

and after some calculations we arrive at

$$\Phi_R(r) = 2\pi^{1/2} r D_-^{1/2}\{\Phi_1(x^{1/2})\}(r^2), \tag{14}$$

where $D_-^{1/2}$ is the right-side Riemann-Liouville fractional derivative of order $1/2$ [26]:

$$D_-^{1/2}\{f(x)\}(y) = -\frac{d}{dy}\frac{1}{\pi^{1/2}}\int_y^\infty \frac{f(x)}{(x-y)^{1/2}}dx. \tag{15}$$

This fractional derivative can be calculated numerically; for instance, see Ref. [27] for Matlab code. Combining Eqs. (9) and (14) gives us

$$\Phi_R(r) = -\frac{2r}{\pi^{1/2}}D_-^{1/2}\left\{\frac{1}{x^{1/2}}\,\mathrm{Im}\,\frac{{}_2F_1\big([1-\alpha]/2,1-\alpha/2;1;\frac{1}{x}\big)}{{}_2F_1\big(-\alpha/2,[1-\alpha]/2;1;\frac{1}{x}\big)}\right\}(r^2)$$

if $r \in (0,1)$ and $\Phi_R(r) = 0$ otherwise. In Cartesian coordinates $H(\mathbf{x},t)$ can be calculated as

$$H(\mathbf{x},t) = \frac{1}{2\pi t\|\mathbf{x}\|}\Phi_R\left(\frac{\|\mathbf{x}\|}{t}\right) \tag{16}$$

with $\|\mathbf{x}\| = \sqrt{x_1^2+x_2^2}$. Therefore

$$H(\mathbf{x},t) = -\frac{1}{\pi^{3/2}t^2}D_-^{1/2}\left\{\frac{1}{x^{1/2}}\,\mathrm{Im}\,\frac{{}_2F_1\big([1-\alpha]/2,1-\alpha/2;1;\frac{1}{x}\big)}{{}_2F_1\big(-\alpha/2,[1-\alpha]/2;1;\frac{1}{x}\big)}\right\}\left(\frac{\|\mathbf{x}\|^2}{t^2}\right) \tag{17}$$

for $\|\mathbf{x}\| < t$ and $H(\mathbf{x},t) = 0$ in the opposite case. Figure 1(b) shows $H(\mathbf{x},1)$ for $\alpha = 0.6$ calculated from Eq. (17). The result is in agreement with the density pictured in Fig. 1(a) estimated using Monte Carlo (MC) methods from 10^7 trajectories. The algorithm for simulating Lévy walks is shown in Appendix C (see also Ref. [28]). The right panel of Fig. 1 shows that $H(\mathbf{x},1) \to \infty$ when $\|\mathbf{x}\| \to 1$, and MC methods reveal it only after a large number of simulations, which is time-consuming.

B. 3D case

For the 3D process $\mathbf{X}(t) = (X_1(t),X_2(t),X_3(t))$ we use the same procedure as for the 2D case. The notation remains the same. The random vectors $\mathbf{V}_i$ have uniform distribution $K(d\mathbf{u})$ on the sphere $\mathbf{S}^3$. The Fourier-Laplace transform of $H(\mathbf{x},t),\mathbf{x} = (x_1,x_2,x_3)$, is [18]

$$H(\mathbf{k},s) = \frac{1}{s}\frac{\int_{\mathbf{S}^3}\big(1-\big\langle\frac{i\mathbf{k}}{s},\mathbf{u}\big\rangle\big)^{\alpha-1}K(d\mathbf{u})}{\int_{\mathbf{S}^3}\big(1-\big\langle\frac{i\mathbf{k}}{s},\mathbf{u}\big\rangle\big)^{\alpha}K(d\mathbf{u})}, \tag{18}$$

where $\mathbf{k} = (k_1,k_2,k_3) \in \mathbb{R}^3$ is the Fourier space variable, s is the Laplace space variable, and $\langle\ ,\ \rangle$ denotes the inner product in $\mathbb{R}^3$. Surprisingly enough, applying the same reasoning as in the 2D case we arrive at much simpler results. This is caused by the fact that the 1D marginal distribution $K_1(du_1)$ of $K(d\mathbf{u})$ is uniform on the interval $[-1,1]$ [24]. Following the reasoning from the 2D case we obtain that the distribution $\Phi_1(x)$ of $X_1(1)$ is expressed in terms of elementary functions

$$\Phi_1(x) = \frac{2(\alpha+1)}{\pi\alpha}\sin(\pi\alpha)\frac{(1-x^2)^\alpha}{(1-x)^{2\alpha+2}+(1+x)^{2\alpha+2}+2\cos(\pi\alpha)(1-x^2)^{\alpha+1}}$$

for $x \in (-1,1)$ and $\Phi_1(x) = 0$ otherwise. Equation (12) now has the form

$$\mathbf{P}(|X_1(1)| \leqslant x) = \int_0^1 \mathbf{P}\Big(\|\mathbf{X}(1)\| \leqslant \frac{x}{u}\Big)du, \tag{19}$$

and the following relation between Φ_R and Φ_1 holds:

$$\Phi_R(r) = -2r\Phi_1'(r). \tag{20}$$

Therefore

$$\Phi_R(r) = \frac{8}{\pi}\frac{\alpha+1}{\alpha}\sin(\pi\alpha)r(1-r^2)^{\alpha-1}\frac{(1+r)^{2+2\alpha}(1+\alpha-r)-(1-r)^{2+2\alpha}(1+\alpha+r)-2r(1-r^2)^{1+\alpha}\cos(\pi\alpha)}{[(1+r)^{2+2\alpha}+(1-r)^{2+2\alpha}+2(1-r^2)^{1+\alpha}\cos(\pi\alpha)]^2} \tag{21}$$

for $r \in (0,1)$ and $\Phi_R(r) = 0$ in the opposite case. Coming back to Cartesian coordinates we get

$$H(\mathbf{x},t) = \frac{1}{4\pi t\|\mathbf{x}\|^2}\Phi_R\left(\frac{\|\mathbf{x}\|}{t}\right), \tag{22}$$

with $\|\mathbf{x}\|=\sqrt{x_1^2+x_2^2+x_3^2}$. Figure 2 presents $\Phi_R(r)$ for different values of α calculated from Eq. (21). We notice that the theoretical results are in perfect agreement with simulations. For the Monte Carlo method we generated 10^5 trajectories of Lévy walk $\mathbf{L}(t)$ with different values of α. Then we plotted the empirical PDF of $\frac{1}{t}\|\mathbf{L}(t)\|$, where the values of t were 10^8, 10^6, and 10^4 for α equal to 0.2, 0.5, and 0.8 respectively. Recall that the PDF of $\frac{1}{t}\mathbf{L}(t)$ converges to the PDF of $\mathbf{X}(1)$ when $t \to \infty$. The simulations, done in Matlab 2014a running on a 2.7 GHz Intel Core i5-5200U CPU, required 2 h 15 min to complete. The required time increases when we take greater values of t.

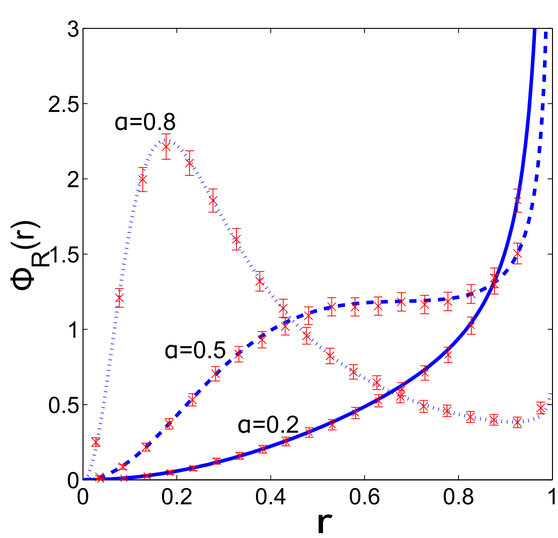

FIG. 2. Density $\Phi_R(r)$ of 3D Lévy walk obtained from Eq. (21) for $\alpha = 0.2, \alpha = 0.5$, and $\alpha = 0.8$ (blue lines). Theoretical results are compared with densities estimated using Monte Carlo methods (red crosses with error bars).

III. CONCLUSIONS

Concluding, in this paper we derived the explicit formulas for the densities of 2D and 3D ballistic Lévy walk limits. The results have a simple form, especially in the 3D case. The methods presented here can be successfully applied to different types of Lévy walks operating in a ballistic regime. Furthermore, the same techniques allow us to calculate the PDF of d-dimensional Lévy walks where the number of dimensions d is arbitrary. We believe that our result will prove useful in practical applications of Lévy walks. In particular it should simplify the verification procedure and estimation of the parameters of the model and give deeper understanding of the properties of Lévy walks.

ACKNOWLEDGMENTS

The authors thank Vasily Zaburdaev for interesting discussions on this topic. This research was partially supported by NCN Maestro Grant No. 2012/06/A/ST1/00258.

APPENDIX A: FOURIER-LAPLACE TRANSFORM OF THE SCALING FUNCTION g_1

The Fourier-Laplace transform of $H_1(x,t)$ is defined as

$$H_1(k,s) = \int_{-\infty}^{\infty}\int_0^{\infty} e^{-ikx-st}H_1(x,t)\,dt\,dx \tag{A1}$$

$$= \int_{-\infty}^{\infty}\int_0^{\infty} e^{-ikx-st}\frac{1}{t}\Phi_1\Big(\frac{x}{t}\Big)dt\,dx. \tag{A2}$$

The substitution $y = \frac{x}{t}$ yields

$$H_1(k,s) = \int_{-\infty}^{\infty}\int_0^{\infty} e^{-(iky+s)t}\Phi_1(y)dt\,dy \tag{A3}$$

$$= \int_{-\infty}^{\infty}\frac{1}{iky+s}\Phi_1(y)dy = \frac{1}{s}\int_{-\infty}^{\infty}\frac{1}{\frac{ik}{s}y+1}\Phi_1(y)dy \tag{A4}$$

$$= \frac{1}{s}\mathbf{E}\frac{1}{\frac{ik}{s}X_1(1)+1}, \tag{A5}$$

justifying Eq. (5).

APPENDIX B: APPLICATION OF SOKHOTSKY-WEIERSTRASS THEOREM

The density $\Phi_1(x)$ can be written as

$$\Phi_1(x) = \mathbf{E}\delta[x - X_1(1)]. \tag{B1}$$

The Sokhotsky-Weierstrass theorem assures us that

$$\lim_{\varepsilon\to 0} \frac{1}{x \pm i\varepsilon} = \frac{1}{x} \mp i\pi\delta(x) \tag{B2}$$

which implies

$$\delta(x) = -\operatorname{Im}\lim_{\varepsilon\to 0} \frac{1}{x + i\varepsilon}. \tag{B3}$$

From Eqs. (B1) and (B3) we obtain

$$\Phi_1(x) = -\operatorname{Im}\lim_{\varepsilon\to 0} \mathbf{E}\frac{1}{x - X_1(1) + i\varepsilon} \tag{B4}$$

$$= -\lim_{\varepsilon\to 0}\operatorname{Im}\left[\frac{1}{x+i\varepsilon}\mathbf{E}\frac{1}{1-\frac{X_1(1)}{x+i\varepsilon}}\right], \tag{B5}$$

which proves Eq. (6).

APPENDIX C: NUMERICAL SIMULATION OF MULTIDIMENSIONAL Lévy WALKS

Below we present the algorithm for simulation of trajectories of $\mathbf{L}(s)$ on a time interval $[0,t]$.

(1) Simulate the sequence of IID random variables T_i for $i = 1,2,\dots,N(t)+1$ where T_i have a one-sided positive α-stable distribution and $N(t) = \max\{k \geqslant 0 \ : \ \sum_{i=1}^{k} T_i \leqslant t\}$. For generating T_i one can use the following procedure [17]:

$$T_i = \frac{\sin[\alpha(V+\pi/2)]}{[\cos(V)]^{1/\alpha}}\left\{\frac{\cos[V - \alpha(V+\pi/2)]}{W}\right\}^{(1-\alpha)/\alpha}, \tag{C1}$$

where the random variable V is uniformly distributed on $(-\pi/2,\pi/2)$ and W has an exponential distribution with mean one. Moreover V and W are assumed to be independent.

(2) Simulate the sequence of IID random vectors $\mathbf{V}_i$ independent from T_i for $i = 1,2,\dots,N(t)+1$ where V_i are uniformly distributed on a circle (2D case) or a sphere (3D case). For the 2D case we generate

$$\mathbf{V}_i = [\cos(U), \sin(U)], \tag{C2}$$

where U has a uniform distribution on a interval $(0,2\pi)$. For the 3D case we generate

$$\mathbf{V}_i = \frac{1}{\sqrt{Z_1^2+Z_2^2+Z_3^2}}[Z_1,Z_2,Z_3], \tag{C3}$$

where Z_i are independent and have a normal distribution $\mathcal{N}(0,1)$. Alternatively one can use rejection sampling.

(3) Set

$$N\left(\frac{kt}{n}\right) = \max\left\{k \geqslant 0 \ : \ \sum_{i=1}^{k} T_i \leqslant \frac{kt}{n}\right\} \tag{C4}$$

for $k = 0,1,2,\dots,n$.

(4) Finally $\mathbf{L}(\frac{kt}{n})$ for $k = 0,1,2,\dots,n$ is calculated directly from its definition given by Eq. (1):

$$\mathbf{L}\left(\frac{kt}{n}\right) = \sum_{i=1}^{N(\frac{kt}{n})} T_i\mathbf{V}_i + \left(t - \sum_{i=1}^{N(\frac{kt}{n})} T_i\right)\mathbf{V}_{N(\frac{kt}{n})+1}. \tag{C5}$$

[1] M. F. Shlesinger, J. Klafter, and Y. M Wong, J. Stat. Phys. **27**, 499 (1982).
[2] J. Klafter, A. Blumen, and M. F. Shlesinger, Phys. Rev. A **35**, 3081 (1987).
[3] G. Margolin and E. Barkai, Phys. Rev. Lett. **94**, 080601 (2005).
[4] P. Barthelemy, P. J. Bertolotti, and D. S. Wiersma, Nature (London) **453**, 495 (2008).
[5] W. J. Bell, *Searching Behaviour: The Behavioural Ecology of Finding Resources* (Chapman and Hall, London, 1991).
[6] H. C. Berg, *Random Walks in Biology* (Princeton University Press, Princeton, 1993).
[7] M. Buchanan, Nature (London) **453**, 714 (2008).
[8] D. Brockmann, in *Reviews of Nonlinear Dynamics and Complexity*, edited by H. G. Schuster (Wiley-VCH, Weinheim, 2009), Vol. 2.
[9] B. Dybiec, Phys. A **387**, 4863 (2008).
[10] T. H. Solomon, E. R. Weeks, and H. L. Swinney, Phys. Rev. Lett. **71**, 3975 (1993).
[11] D. Brockmann, L. Hufnagel, and T. Geisel, Nature (London) **439**, 462 (2006).
[12] M. C. Gonzales, C. A. Hidalgo, and A. L. Barabasi, Nature (London) **453**, 779 (2008).
[13] G. Ariel, A. Rabani, S. Benisty, J. D. Partridge, R. M. Harshey, and A. Be'er, Nature Comm. **6**, 8396 (2015).
[14] V. Zaburdaev, S. Denisov, and J. Klafter, Rev. Mod. Phys. **87**, 483 (2015).
[15] J. Klafter and I. M. Sokolov, *First Steps in Random Walks: From Tools to Applications* (Oxford University Press, Oxford, 2011).
[16] R. Metzler and J. Klafter, Phys. Rep. **339**, 1 (2000).
[17] A. Janicki and A. Weron, *Simulation and Chaotic Behavior of α-Stable Stochastic Processes* (Dekker, New York, 1994).
[18] M. Magdziarz, H. P. Scheffler, P. Straka, and P. Zebrowski, Stoch. Proc. Appl. **125**, 4021 (2015).
[19] I. M. Sokolov and R. Metzler, Phys. Rev. E **67**, 010101(R) (2003).
[20] V. V. Uchaikin and R. T. Sibatov, J. Phys. A: Math. Theor. **44**, 145501 (2011).
[21] V. V. Uchaikin and V. M. Zolotarev, *Chance and Stability: Stable Distributions and Their Applications* (De Gruyter, Utrecht, 1999).
[22] C. Godreche and J. M. Luck, J. Stat. Phys. **104**, 489 (2001).

[23] D. Froemberg, M. Schmiedeberg, E. Barkai, and V. Zaburdaev, Phys. Rev. E **91**, 022131 (2015).

[24] W. Feller, *An Introduction to Probability Theory and Its Applications*, Vol. 2 (Wiley, New York, 1971).

[25] M. Abramowitz and I. A. Stegun, Hypergeometric functions, in *Handbook of Mathematical Functions with Formulas, Graphs, and Mathematical Tables* (Dover, New York, 1972), pp. 555–566.

[26] A. A. Kilbas, H. M. Srivastava, and J. J. Trujillo, *Theory and Applications of Fractional Differential Equations* (North-Holland Mathematics Studies, Amsterdam, 2006).

[27] I. Podlubny, http://www.mathworks.com/matlabcentral/fileexchange/22071.

[28] M. Magdziarz and M. Teuerle, Commun. Nonlinear Sci. Numer. Simul. **20**, 489 (2015).